ELSEVIER

Physics of the Earth and Planetary Interiors 101 (1997) 119–130

PHYSICS OF THE EARTH AND PLANETARY INTERIORS

The non-linear initiation of diapirs and plume heads

David Bercovici *, Amanda Kelly

Department of Geology and Geophysics, School of Ocean and Earth Science and Technology, University of Hawaii at Manoa, Manoa, HI, USA

Received 25 April 1996; accepted 24 July 1996

Abstract

A simple theory is devised to describe the non-linear feedback mechanisms involved in the initial growth of a single diapir or plume head from a low viscosity channel overlain by a much more viscous layer. Such feedbacks arise primarily from the relation between the growth of a proto-diapir (i.e. an undulation on the upper boundary of the low viscosity channel) and the draining of the low viscosity channel. In the period of time between its initial exponential growth (characterized by linear stability analysis) and its separation from the low viscosity channel as a fully formed diapir, the proto-diapir can undergo a significant cessation in its development due to deflation of the low viscosity channel; i.e. the proto-diapir's growth can essentially stall for a long period of time before it separates and begins its ascent through the overlying medium. The theory is used to determine a criterion for separation of the diapir from the low viscosity channel that is in terms of the geometrical and mechanical properties of the channel, instead of the ad hoc volume flux widely used in many models of mantle plumes and plume heads (e.g. Whitehead and Luther, 1975; Richards et al., 1989; Olson, 1990; Sleep, 1990; Bercovici and Mahoney, 1994). From this separation criterion, self-consistent scaling laws can be formulated to relate the size of the fully developed diapir and its trailing conduit to the properties of the initial channel, instead of to the ad hoc volume flux. Basic laboratory experiments involving highly viscous fluids are presented and demonstrate that the so-called 'stalling' period between initial growth and separation does indeed occur. These results suggest that nascent mantle plume heads may stall for extended periods at the base of the mantle and thereby contribute to variations in thickness of the D″ layer.© 1997 Elsevier Science B.V.

1. Introduction

Diapirism is a prevalent geological phenomenon occurring, for example, in the formation of salt domes, granites and mantle plumes. Diapiric plume heads rising from the D″ layer at the core–mantle boundary (or some other thermal boundary layer at a heated interface) are thought to mark the initiation of mantle plumes and hotspot tracks and have been hypothesized to be the cause of flood basalts (White and McKenzie, 1989; Richards et al., 1989; Campbell and Griffiths, 1990; see also Bercovici and Mahoney, 1994; Farnetani and Richards, 1994). The initiation of a viscous diapir at the interface between two fluids of different viscosity and density is described by linear Rayleigh–Taylor stability theory (Whitehead and Luther, 1975; see Loper and Eltayeb, 1986, and Ribe and de Valpine, 1994, for applications to the D″ layer). After the diapir forms there are simple theories for how the diapir separates from its source region and ascends while being inflated by

* Corresponding author.

PII S0031-9201(96)03217-7

a trailing conduit (Whitehead and Luther, 1975; Olson, 1990). However, there is relatively little understanding of the intermediate stage, when the interface undulation is of finite amplitude (i.e. comparable to the thickness of the source region) and about to coalesce into a fully developed diapir. At this stage, the growth rate of the undulation can possibly diminish, particularly if it significantly drains the local source region.

Apart from numerical experiments (e.g. Christensen, 1984; Olson et al., 1987; Weinberg and Podladchikov, 1995), non-linear and finite amplitude Rayleigh–Taylor instability is typically treated with perturbation theory (Haan, 1989; Fermigier et al., 1992; Cafaro and Cima, 1993; see review by Kull, 1991), which essentially reveals pattern formation and symmetry breaking in a field of undulations. However, a simple theoretical understanding of the non-linear evolution and growth of an isolated undulation, from infinitesimal to finite amplitude, would have significant value. Such a theory is necessary to give a basic estimate for the duration of diapir initiation. Long lived undulations or proto-diapirs will clearly affect the apparent structure of the source region. For example, the time for plume heads to develop in the D″ layer has significant implications regarding observed variations in the structure of the D″ (Kuo and Wu, 1995; see Loper and Lay, 1995) and related effects, such as lateral variations in heat flux out of the core which invariably influence dynamo and geomagnetic activity (Gubbins and Richards, 1986; Larson and Olson, 1991; Loper, 1992; see Loper and Lay, 1995). Since this theory would provide a link between diapir initiation and diapir separation, it would intrinsically yield a more self-consistent framework for relating the physics of fully developed diapirs to the properties of the source region. Most simple theories of fully developed diapirs depend on specifying a volume flux Q into the conduit feeding the diapir (Whitehead and Luther, 1975; Richards et al., 1989; Sleep, 1990; Bercovici and Mahoney, 1994); the length scales of both the plume head and conduit are thus invariably prescribed by the input volume flux Q. Although Q for a mantle plume can be inferred from hotspot mass or heat flux (Davies, 1988; Sleep, 1990) it is not, in fact, a fundamental property of the mantle; Q is really an outcome of the dynamics of the plume head's initiation. In short, Q necessarily depends on the viscosity, buoyancy and the thickness of the source region.

In this paper, we propose and examine a simple non-linear theory that simultaneously models the growth of a single diapir and the shrinkage of the diapir's source region. This theory thus accounts for the growth of a proto-diapir, from an infinitesimal disturbance to a finite amplitude undulation about to separate into a fully developed diapir. We examine the condition for its separation from the source region, and, from this, estimate the initial scales of the starting plume head and its trailing conduit in terms of the properties of the source region. Finally, to test the validity of our theory, we compare our model predictions to some basic laboratory experiments. It should be noted that, strictly speaking, our theoretical and experimental diapirs have only chemical density anomalies which diffuse much less rapidly than do thermal density anomalies. This assumption is clearly appropriate for the formation of salt domes and granitic bodies; however, the extent to which mantle plumes are chemical or thermal is not entirely known, though they are likely to be predominantly thermal.

2. Theory

2.1. Plume-head initiation

At the heart of our model is a simple non-linear feedback mechanism. A dome-shaped disturbance or proto-diapir grows on the interface between a viscous fluid channel and an overlying higher-viscosity, higher-density layer. The disturbance coincides with a pressure low which is mainly due to the buoyant hydrostatic head of the disturbance. Fluid in the lower-viscosity channel flows toward the pressure low, causing the channel to deflate, the dome-shaped disturbance to grow, and the pressure low to increase in magnitude, and so on. Moreover, as the surrounding channel shrinks, flow within it becomes more constricted, limiting the fluid supply to the proto-diapir. Nevertheless, the proto-diapir will grow until its Stokes ascent velocity exceeds its own growth rate, at which point it will separate from the channel (Whitehead and Luther, 1975).

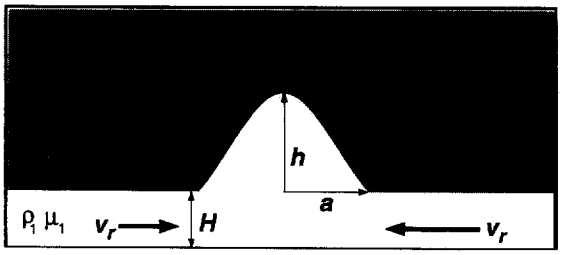

Fig. 1. Sketch of diapir-initiation model. See text for further definition of symbols.

We construct the model to examine a single plume head growing from an initially uniform layer of density ρ_1 and viscosity μ_1 overlain by an infinite half space of higher density ρ_2 and much higher viscosity μ_2 (Fig. 1). We assume the width of the growing plume head $2a$ and its distance from neighboring plume heads $2R$ is determined by linear Rayleigh–Taylor stability theory (Whitehead and Luther, 1975); i.e. both R and a scale as the wavelength of the least stable infinitesimal disturbance. We adopt an axisymmetric geometry centered on the growing plume head and separate the low viscosity layer into two regions. The first region is that of the growing dome-shaped disturbance contained within a radius of $r = a$; the second is the uniformly flat source region between $r = a$ and a stagnation perimeter at $r = R$. (The stagnation perimeter is the line where the suction from other growing diapirs cancels that of the diapir in question; this is not a crucial assumption or feature, but does simplify the model some.) The growing proto-diapir is modelled as a Gaussian-shaped disturbance with a height above the top of the low viscosity layer prescribed by he^{-4r^2/a^2} such that the radius $r = a$ marks the boundary between the growing disturbance and the deflating flat-layer region. The Gaussian shape is justified somewhat by numerical models (e.g. Farnetani and Richards, 1995) and our laboratory experiments (see below). The maximum height h grows with time, though a is assumed to stay constant. (The constancy of a is based on the assumption that as the disturbance grows it is free to rise and extend vertically since it is buoyant and unbounded from above; it will thus not spread laterally like a gravity current. The constant-a assumption, however, clearly does not hold when the diapir separates from the source region and develops a tail.) The flat layer region surrounding the plume head has height H which diminishes with time as the plume head grows. Since $\mu_2 \gg \mu_1$, linear stability theory prescribes both a and R to be proportional to $(\mu_2/\mu_1)^{1/3}H_0$ where H_0 is the initial, undisturbed channel thickness, i.e. H at time $t = 0$.

In the flat low-viscosity channel region ($a \le r \le R$, $0 \le z \le H$), there is primarily radial flow with velocity v_r; we employ shallow-layer lubrication theory to obtain the radial volume flux per unit length

$$q = \int_0^H v_r \mathrm{d}z = \frac{H^3}{3\mu_1}\frac{\partial P}{\partial r} \tag{1}$$

where P is pressure, to be defined shortly. We have assumed that the interface with the overlying highly viscous medium is effectively a no-slip boundary, while the bottom boundary of the channel is assumed free-slip, as appropriate for the core–mantle boundary of the Earth; a no-slip bottom boundary would simply require multiplying the right side of Eq. (1) by $1/4$. By continuity

$$\frac{\partial H}{\partial t} = -\frac{1}{r}\frac{\partial}{\partial r}(rq) \tag{2}$$

However, in our simple model H is assumed independent of r, thus, by Eqs. (1) and (2),

$$\frac{\partial}{\partial r}\left(\frac{1}{r}\frac{\partial}{\partial r}\left(r\frac{\partial P}{\partial r}\right)\right) = 0 \tag{3}$$

We apply the boundary conditions that

$$P = P_0 \text{ at } r = R \tag{4}$$

where P_0 is the over-burden pressure,

$$\frac{\partial P}{\partial r} = 0 \text{ at } r = R \tag{5}$$

since $r = R$ is an assumed stagnation point, and

$$P = P_0 - f(\Delta\rho g h - p') \text{ at } r = a \tag{6}$$

where $\Delta\rho = \rho_2 - \rho_1$; p' is the dynamic pressure opposing the inflation of the plume head due to motion of the overlying viscous medium; and f is some fraction ≤ 1 (see Appendix A) to account for the fact that we are measuring the pressure at $r = a$

not $r = 0$. Given these conditions, the pressure is given by

$$P = P_0 - f\frac{Y(r)}{Y(a)}(\Delta\rho g h - p') \tag{7}$$

where

$$Y(r) = r^2/R^2 + 2\log(R/r) - 1 \tag{8}$$

The opposing pressure p' from the overlying medium is not easily determined in the case of a finite value of h (i.e. where h is not $\ll H$). The two limiting forms of the plume head are (1) when the disturbance is infinitesimal and (2) when the plume head is nearly a diapir ready to separate. In either case, the pressure opposing vertical motion is of the form $p' = c\mu_2 W/a$ (Batchelor, 1967) where W is the absolute vertical velocity of the interface, i.e. $W = (\mathrm{d}/\mathrm{d}t)(h + H)$ and c is some constant probably between 3 and 2π (Batchelor, 1967; Whitehead and Luther, 1975; Turcotte and Schubert, 1982) (also see the following section for reasons why a alone is assumed the relevant length scale in p'). For the sake of simplicity and consistency with the limiting states of the plume head, we adopt this form of p' in the present analysis, i.e.

$$p' = c\frac{\mu_2}{a}\frac{\mathrm{d}}{\mathrm{d}t}(h + H) \tag{9}$$

The deflation of the flat channel surrounding the growing plume head is given by Eq. (2), which, using Eqs. (1), (7)–(9), leads to

$$\frac{\mathrm{d}H}{\mathrm{d}t} = -\frac{4f}{3\mu_1 R^2 Y(a)}H^3 \times\left(\Delta\rho g h - c\frac{\mu_2}{a}\frac{\mathrm{d}(h+H)}{\mathrm{d}t}\right) \tag{10}$$

By conservation of mass, the growth in volume of the plume head is given by

$$\frac{\mathrm{d}}{\mathrm{d}t}\left[2\pi\int_0^a h e^{-4r^2/a^2} r\,\mathrm{d}r + \pi a^2 H\right] = -2\pi a q(a) \tag{11}$$

which, with Eq. (1) and Eqs. (7)–(10), leads to

$$\frac{\mathrm{d}h}{\mathrm{d}t} = \frac{2f}{3\gamma\mu_1 a^2 Y(a)}H^3\left(\Delta\rho g h - c\frac{\mu_2}{a}\frac{\mathrm{d}(h+H)}{\mathrm{d}t}\right) \tag{12}$$

where $\gamma = \frac{1}{8}(1 - e^{-4})$. (Note that $Y(a) > 0$ for all $a < R$.) We non-dimensionalize H by its initial value H_0, time by

$$t_0 = \frac{c\mu_2}{\Delta\rho g a} \tag{13}$$

(which is comparable to the time for the fully developed diapir to traverse is own girth) and h by

$$h_0 = \frac{3Y(a)}{4fc}\frac{\mu_1}{\mu_2}\frac{R^2 a}{H_0^2} \tag{14}$$

(which follows a posteriori from the scaling factors H_0 and t_0). By dividing the dimensionless version of Eq. (10) by that of Eq. (12), and using the initial conditions (on the dimensionless quantities) that

$$H = 1 \text{ and } h = \epsilon \text{ at } t = 0 \tag{15}$$

we obtain

$$H = \frac{\lambda + \epsilon - h}{\lambda}; \tag{16}$$

substitution of this expression for H into the dimensionless version of Eq. (12) leads to an integrable non-linear evolution equation for h

$$\frac{\mathrm{d}h}{\mathrm{d}t} = \frac{h(\lambda + \epsilon - h)^3}{\lambda^2 + \nu(\lambda + \epsilon - h)^3} \tag{17}$$

where

$$\lambda = \frac{2fc}{3\gamma Y(a)}\frac{\mu_2}{\mu_1}\frac{H_0^3}{a^3} \tag{18}$$

and

$$\nu = 1 - \frac{H_0}{\lambda h_0} = 1 - 2\gamma\frac{a^2}{R^2} \tag{19}$$

Typical values for the parameter λ lie between 10 and 1000 (see Appendix A) where the smaller λ corresponds to large values of a/R and large λ are associated with smaller a/R. For most proto-diapirs we expect $a/R \approx 1/2$ which corresponds to a value of λ that is $O(10)$. The parameter ν does not vary significantly, i.e. $0.75 < \nu < 1.0$.

Fig. 2 shows $\mathrm{d}h/\mathrm{d}t$ versus h for several values of λ (with $\epsilon = 10^{-2}$ and $\nu = 0.9$). Initially, $\mathrm{d}h/\mathrm{d}t$ increases linearly with h, which is indicative of

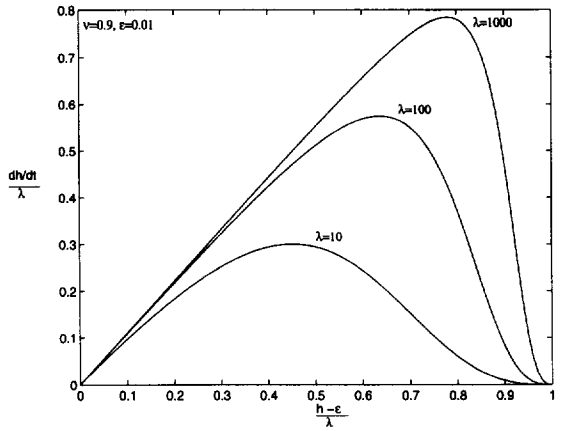

Fig. 2. Curves of dh/dt versus h from Eq. (17) for three values of λ. For all three cases $\nu = 0.9$ and $\epsilon = 0.01$.

exponential growth in h; however, dh/dt eventually reaches a maximum when

$$\nu(\lambda + \epsilon - h)^4 + \lambda^2(\lambda + \epsilon - 4h) = 0 \qquad (20)$$

and goes to zero when $h = \lambda + \epsilon$. Therefore, h achieves a maximum of $\lambda + \epsilon$ since its growth rate vanishes when it reaches this value. Obviously, this is the value of h whence $H = 0$ (see Eq. (16)), i.e. when the source region is entirely depleted. Moreover, note that λ controls the final value of h because it determines the width of the undulation (e.g. large λ means small a/R); i.e. if the entire volume of the source region (to the stagnation perimeter) is drained into the undulation, then obviously a narrow undulation will grow to a greater height than a broad one.

The dynamical equation for undulation height, i.e. Eq. (17), can be integrated, with the constraints of Eq. (15), to yield an implicit analytic solution for h:

$$t = \nu \log(h/\epsilon) + \frac{\lambda^2}{(\lambda+\epsilon)^3}\log\left(\frac{\lambda h/\epsilon}{\lambda+\epsilon-h}\right) + \frac{\lambda^2}{\lambda+\epsilon}\left(\frac{1}{2(\lambda+\epsilon-h)^2} - \frac{1}{2\lambda^2} + \frac{1}{(\lambda+\epsilon)(\lambda+\epsilon-h)} - \frac{1}{(\lambda+\epsilon)\lambda}\right) \qquad (21)$$

Fig. 3 of h versus t shows initially gradual growth of the plume head, followed by rapid (exponential) inflation and, finally, a levelling of the inflation rate as the plume head's supply becomes depleted. However, after a certain time, the plume head necessarily separates from the source layer; this separation is indicated by the change to positive curvature in the h-versus-t curve (see Section 2.2 and Appendix B).

2.2. Plume-head separation

We wish to examine the conditions whereby the proto-diapir separates from the channel or source region; this will allow us to estimate the duration of

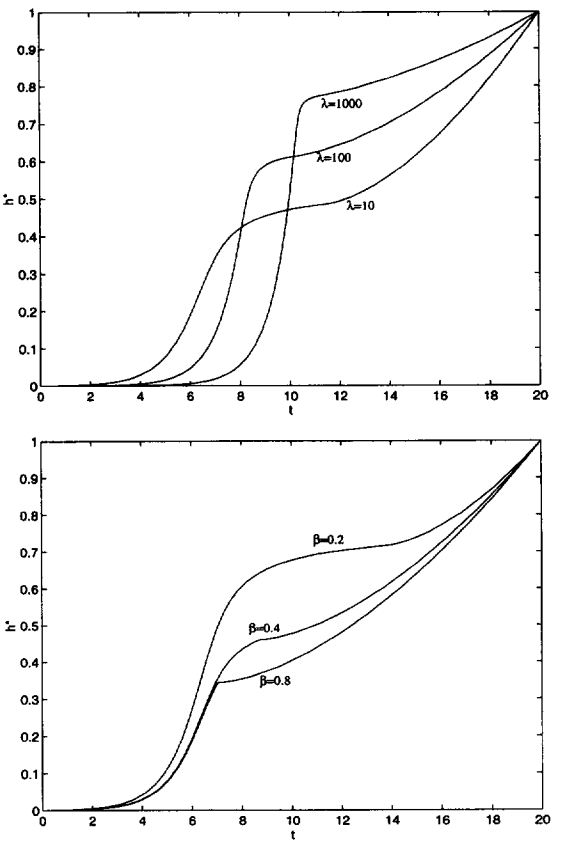

Fig. 3. Curves of $h^* = (h - \epsilon)/(h_{max} - \epsilon)$ (where h_{max} is the maximum h calculated, i.e. h at the final time) versus dimensionless time t for various values of λ (indicated on the figure) with $\beta = 0.25$ (top frame) and various values of β (indicated on the figure) with $\lambda = 10$ (bottom frame). These calculations use Eq. (17) or Eq. (21) for plume growth prior to separation (i.e. for $t \le t_{sep}$) with $\nu = 0.9$, $\epsilon = 0.01$ (see text and Appendix A for discussion of dimensionless parameters). After separation ($t \ge t_{sep}$) the curves obey Eq. (B2) with $\alpha = 2$ (see Appendix B).

the period between its initial exponential growth and its separation into a fully developed diapir. We can also obtain a separation criterion in terms of viscosities and initial channel thickness, instead of in terms of an ad hoc plume volume flux Q (Whitehead and Luther, 1975). Moreover, we can infer the sizes of the trailing conduit and diapir at the point of separation, independent of Q.

We expect separation to occur when the Stokes or free ascent velocity W_s of the forming diapir exceeds its growth rate $(\mathrm{d}(h+H)/\mathrm{d}t)$ (Whitehead and Luther, 1975). The effective resistive viscous force on the freely ascending diapir is approximately $\Omega\mu_2 aW_s$, where Ω is essentially a solid angle determined by the effective surface area on which the force acts (Batchelor, 1967); for a perfect sphere surrounded by an infinite viscous medium $\Omega = 4\pi$. The primary length scale in the resistive force is assumed to be a since the pressure and normal stress act downward effectively on the horizontal cross-section of the plume head while traction along the vertical sides of the plume head is negligible since $\mu_1 \ll \mu_2$. Therefore, we expect h to play very little role in the scale of the resistive force. (This is also the rationale used in obtaining Eq. (9).) The buoyancy force is $2\pi\gamma a^2 h_0 h \Delta\rho g$ (where we continue to use dimensionless h) and the Stokes velocity is then

$$W_s = \frac{2\pi\gamma\Delta\rho g a h_0 h}{\Omega\mu_2} \tag{22}$$

Separation occurs when

$$\frac{h_0}{t_0}\frac{\mathrm{d}}{\mathrm{d}t}\left(h + \frac{H_0}{h_0}H\right) \le W_s \tag{23}$$

In dimensionless form this becomes

$$\frac{\mathrm{d}h}{\mathrm{d}t} \le \frac{2\pi\gamma c}{\Omega\nu}h \tag{24}$$

Using Eq. (17), separation occurs when

$$h \ge h_{sep} = \lambda + \epsilon - \beta\lambda^{2/3} \tag{25}$$

where

$$\beta = \left(\frac{2\pi\gamma c}{\nu(\Omega - 2\pi\gamma c)}\right)^{1/3} \tag{26}$$

To evaluate the sign of β, we consider that (1) c is no larger than 2π (and actually reduces to the order of 3 when the proto-diapir is large and about to separate); (2) $\gamma = 0.1227$; and (3) Ω is probably between 2π and 4π (since the low viscosity source region underlying the diapir could reduce by as much as half the effective surface area on which stresses in the overlying viscous medium can act). This implies that $\beta > 0$ and thus $h_{sep} < \lambda + \epsilon$, i.e. separation will, with reasonable certainty, occur before h reaches its maximum size of $\lambda + \epsilon$. The time from initiation to separation t_{sep} can be determined by substituting h_{sep} into Eq. (21).

Fig. 3 shows the growth of the undulation to the separation point for various reasonable values of β and λ. Separation occurs at the second inflexion point in each curve, i.e. where curvature goes from negative to positive as h resumes its growth after an effective stalling period. After separation (i.e. $t > t_{sep}$) h represents the height to the top of the rising diapir which continues to be inflated by the trailing conduit (see Appendix B). The stalling period in the growth of the proto-diapir lasts between approximately 1 and 5 dimensionless time units (recall that t_0 from Eq. (13) is the dimensional time scale).

2.3. Size of the separated diapir and trailing conduit

By conservation of mass, the volume flux Q into the diapir at the time of its separation balances the deflation rate of the flat channel, i.e.

$$Q = -\pi R^2 H_0 \left.\frac{\mathrm{d}H}{\mathrm{d}t}\right|_{t_{sep}} = \frac{\pi R^2 H_0 \Delta\rho g a}{c\mu_2}\frac{\beta^3(\lambda + \epsilon - \beta\lambda^{2/3})}{\lambda(1 + \nu\beta^3)} \tag{27}$$

Assuming Poiseuille flow in the trailing conduit, we estimate its radius after the plume head separates to be

$$b = \left(\frac{8Q\mu_1}{\pi\Delta\rho g}\right)^{1/4} \tag{28}$$

Moreover, the initial volume of the plume head, i.e. at separation, is

$$V_i = 2\gamma\pi a^2 h_0 h = \frac{3\pi\gamma Y(a)}{2fc}\frac{\mu_1}{\mu_2}\frac{R^2 a^3}{H_0^2}(\lambda + \epsilon - \beta\lambda^{2/3}) \tag{29}$$

We can now obtain some basic scaling relationships for the conduit radius and plume head size in terms of the viscosity contrast (μ_1/μ_2) and the linear dimensions H_0, R and a. The conduit radius follows the scale relationship of

$$\frac{b^4}{H_0^4} \sim \frac{\mu_1}{\mu_2}\frac{R^2 a}{H_0^3} \tag{30}$$

and the initial plume head volume obeys

$$\frac{V_i}{\pi R^2 H_0} \sim \frac{\mu_1}{\mu_2}\frac{R^3}{H_0^3} \tag{31}$$

where we have used terms of highest order in λ and also the dependence of λ on a/R (see Appendix A). These may be simplified by noting that $a \propto R$ and by linear stability theory $R/H_0 \sim (\mu_2/\mu_1)^{1/3}$; thus,

$$b \sim H_0 \tag{32}$$

and

$$V_i \sim \left(\frac{\mu_2}{\mu_1}\right)^{2/3} H_0^3 \tag{33}$$

The above scaling relationships suggest that while the trailing conduit is as narrow as the source region, the volume of the separated diapir or plume head may be much larger than H_0^3; i.e. the radius of the diapir will be significantly larger than the radius of the conduit. This gives a rigorous basis for addressing one of the more classical questions of mantle plumes, i.e. why a starting plume head is much wider than the plume itself, without appealing to an ad hoc volume flux Q.

3. Laboratory experiments

One of the more intriguing suggestions of the non-linear theory presented here is that between the exponential growth of the initial infinitesimal undulations and the free ascent of a fully developed diapir

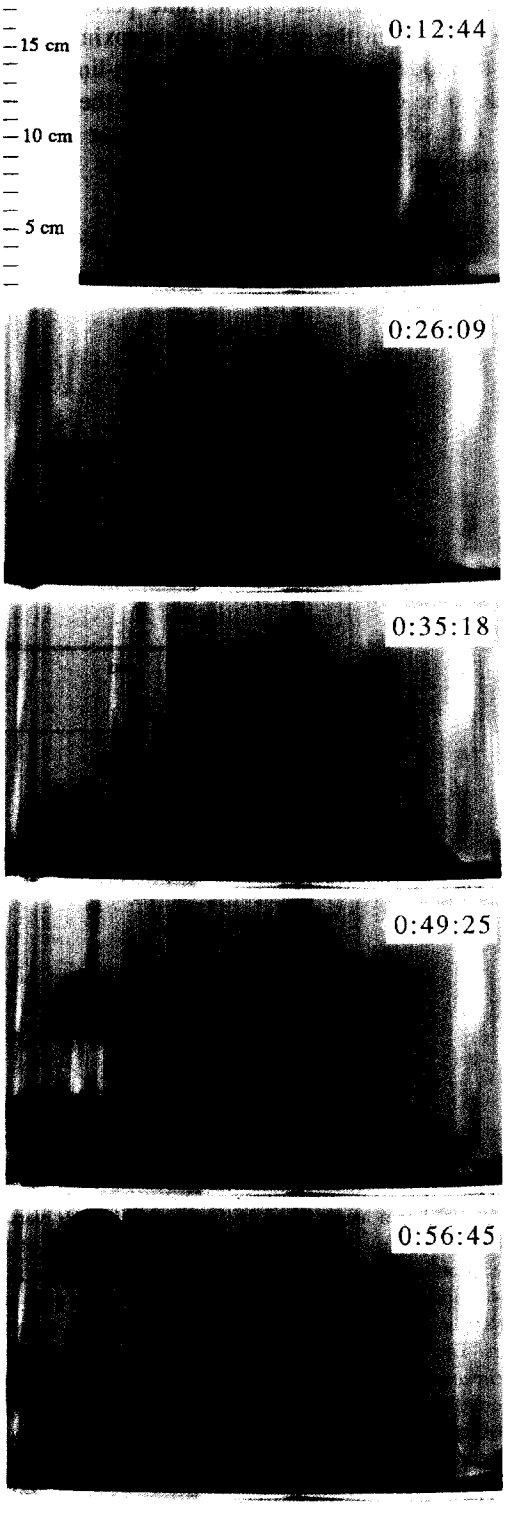

Fig. 4. Photographs of a laboratory experiment showing the initiation and growth of undulations on an interface between two different layers of corn syrup (i.e. a high viscosity layer overlying a much thinner layer of lower viscosity and density). Times and scale are indicated. See text for discussion of experimental details.

are feedback effects which potentially cause the diapir formation to stall for a finite period of time. However, given the simple and approximate nature of our model, this feature of the non-linear theory needs to be experimentally tested. We therefore carried out several basic Rayleigh–Taylor laboratory experiments and measured undulation height for many individual diapirs during their development and ascent.

Laboratory experiments were conducted in an acrylic cylindrical tank with an outer diameter of 30.75 cm, an inner diameter of 29.8 cm and a height of 30.5 cm with its lid. The tank was filled to a height of 28.8 cm with highly viscous corn syrup

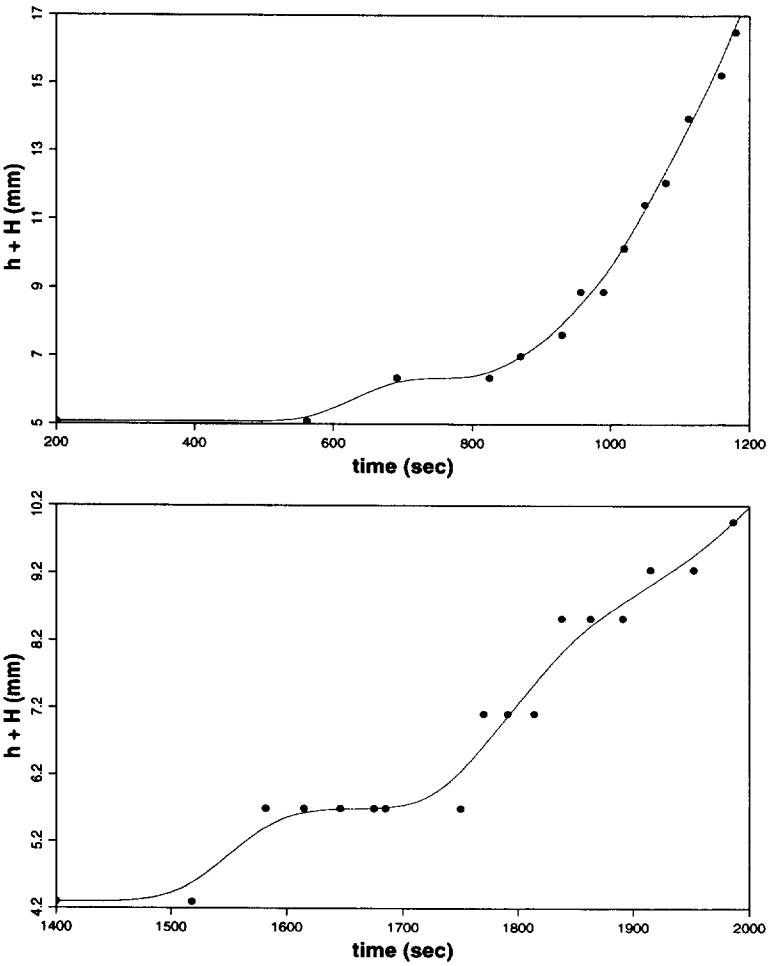

Fig. 5. Undulation height from the tank bottom $h + H$ versus time for selected laboratory diapirs (shown in Fig. 4). These diapirs were chosen to exemplify the stalling period in diapir growth; other experiments showed both comparable and smaller stalling periods. The top frame records the growth of one of the first diapirs in the given experiment; these diapirs arise from a 5-mm-thick layer and are thus the largest diapirs to form. The bottom frame records one of the later secondary diapirs (in the same experiment, shown in Fig. 4 behind the first diapirs); the secondary diapirs are significantly smaller as they arise from a layer that is deflated to approximately 4 mm by the first field of diapirs. The apparent repeated leveling of the data in the bottom frame is due to the fact that the resolution of the photographs of the experiments and the maximum available precision of the measurements of height were not sufficient to precisely track the boundary between the two fluids during the exceedingly slow growth and ascent of the smaller diapirs. This problem with our measurements undoubtedly influences the apparent duration of the stalling period between 1550 and 1750 s. Thus, to reduce measurement bias, both data sets were fit to curves (solid lines) based on smoothing (i.e. convolution filtering) the data consistently with a Gaussian filter with a 200 s full width.

(LSI Specialty Products Liquidose No. 444) which has a density of 1460 kg m^{-3} and a viscosity of 607 330 cP (where cP is centipoise, and 1 cp = 10^{-3} Pa s). On top of this was added a 5-mm layer of lighter and less viscous Karo corn syrup (died purple to enhance its visibility) with a density of 1320 kg m^{-3} and a viscosity of 3839 cP. The viscosity contrast between these fluids is approximately 160 and the density contrast is 1.1. As the two fluids are entirely miscible, capillary forces are negligible. The tank was allowed to sit for approximately 12 h to permit air bubbles to escape and to ensure that the fluid layers had uniform thickness. Diffusion between layers over this time period was negligible. The tank was tightly covered during this time to reduce evaporation of water. When the syrups were mostly bubble-free, a thin disk of acrylic, cut to fit into the top of the tank and lined with teflon tape, was placed on the fluid surface. Care was taken so that no air bubbles became trapped during this process. Waterproof tape was used to secure the disk and to prevent leaks when the tank was inverted. After these preparations were made, the lid was put on the tank and the tank was inverted, so that the 5-mm layer of Karo syrup was overlain by the 28.8-cm layer of thicker corn syrup.

After approximately 10 min, the thin buoyant layer began developing undulations where the Karo corn syrup accumulated (Fig. 4). The undulations were approximately 10 mm wide and dome-shaped; they were detectable either by looking level at the lower layer or looking down through the base of the tank where they appeared as regions of enhanced opacity. The first set of diapirs tend to form near the walls of the tank. As these diapirs mature and separate, another set of diapirs formed closer toward the center of the tank; these secondary diapirs were approximately 2/3 the size of the first ones. Over a period of 9 min the initial undulations became bell-shaped. However, after about 20 min their development often appeared to become arrested and the growth of the diapirs stalled (Fig. 5). For the first set of bigger diapirs this stalling period was relatively brief, i.e. between approximately 1 and 2 min. For the second set of smaller diapirs this period was much longer, i.e. between 5 and 10 min. That the stalling period is most pronounced for the smaller diapirs occurs because these diapirs form from a thinner layer that has been depleted by the first diapirs; therefore, the source region is exhausted more rapidly for the secondary diapirs. However, the theoretical model also predicts that the smaller proto-diapirs will stall for longer times since the relevant time scale is proportional to a^{-1} (see Eq. (13)), where a is the undulation radius; thus all processes, from initial growth to stalling to separation and ascent, will take longer for the smaller plumes. Eventually all the undulations gather into diapirs and separate from the bottom source layer. The approximate nature of the theory makes it impossible to carry out a detailed comparison between model and experiment. However, the experiments do verify, in particular through the occurrence of the stalling period in the development of the proto-diapir, that the theoretical model captures the essential physics of finite amplitude diapir and plume head initiation.

4. Discussion and conclusions

4.1. Stalling of plume-head initiation: implications for structure of the D″

The theory and laboratory experiments presented here indicate that after an undulation on an unstable fluid interface begins to grow exponentially from an infinitesimal disturbance, its growth can become arrested for a finite period of time before separating into a fully developed diapir. This stalling period can last between 1 and 5 t_0, where the time scale t_0 is given by Eq. (13). For mantle plume heads arising from the D″ layer, t_0 is between approximately 10 and 50 Myrs (using $3 \le c \le 2\pi$, $\mu_2 = 10^{22}$ Pa s, $\Delta\rho = 40$ kg m^{-3} as a likely lower mantle thermal density anomaly, $g = 10$ m s^{-2} and $a = 100$ km). This implies that proto-plume heads could stall at the D″ for 10 to several 100 million years before separating into fully developed plume heads.

This has likely significance for the structure and dynamics of the D″ layer. Analyses of the structure of the D″ layer suggests that it is not uniform (Olson et al., 1987; Kuo and Wu, 1995; see Loper and Lay, 1995). This may be inferred to be caused by chemical heterogeneity, or thickness variations induced by descending slabs or slab-induced cold currents im-

pinging on the D″. Typically, a narrow plume conduit emanating from the D″ probably would not be large enough to cause a significant change in D″ thickness. Nascent plume heads are traditionally thought to be too buoyant to reside near the D″ for long (given their potential for relatively rapid ascent). However, this study suggests that proto-plume heads may indeed linger near the core–mantle boundary for extended periods of time, thereby inducing relatively long-lived variations in the thickness of the D″. As the D″ is quite possibly the bottom thermal boundary layer of the mantle convection system it provides the primary control on heat flow and release of gravitational potential energy from the core (see Loper and Lay, 1995). Moreover, the D″ possibly has finite electrical conductivity (Jeanloz, 1993; Shankland et al., 1993; cf. Boehler, 1993) and may therefore control the flux and diffusion of magnetic field lines out of the core. Therefore undulations in the thickness of the D″ would impose a laterally heterogeneous thermal and electrical boundary conditions on core magnetoconvection (Gubbins and Richards, 1986; see Loper and Lay, 1995) and thus have a direct influence on the structure and evolution of the geodynamo.

4.2. Scaling of mantle plumes and plume heads

It is typically assumed that one of the more fundamental features of mantle plumes is that starting plume heads are immense in size while their trailing conduits are relatively narrow. The several hundred kilometer radii of plume heads is inferred from the volume of flood basalts (Richards et al., 1989; Mahoney et al., 1993; Bercovici and Mahoney, 1994) while the less than 100 km radius of the trailing conduits is thought to be reflected in the width of hotspot tracks and in that, until possibly recently (Nataf and VanDecar, 1993), plumes could not be seismologically resolved. The classic physical explanation for this difference in size between plume head and conduit is that given a particular volume flux along a mantle plume, the mobility of the leading plume head is constrained by the large viscosity of the surrounding mantle and therefore cannot move until it is inflated by the particular volume flux to a very large size. In contrast, the mobility of the fluid in the conduit is determined by its own lower viscosity, thus permitting greater flow velocities and thereby accommodating the volume flux with a narrow conduit. While this explanation is intuitively appealing it invokes an ad hoc volume flux that is not a fundamental property of the mantle system. In this paper we have presented a simple model of how plume heads form without assumptions of a volume flux; this allows us to infer the scales of the conduit and the plume head purely from the properties of the source region. We find that the plume head indeed obeys a different scaling than the conduit, i.e. the conduit scales as the thickness of the source region, while the plume head radius goes as this thickness multiplied by $(\mu_2/\mu_1)^{2/9}$. The physical explanation for the different scales does not change (i.e. it still depends on the difference in fluid mobility between the conduit and the plume head); however, the theory presented here provides a more self consistent explanation as to why mantle plumes are so much narrower than their starting plume heads.

Acknowledgements

The authors thank Cinzia Farnetani and Peter Olson for helpful reviews, and Neil Frazer who asked the innocent question "why are mantle plumes so narrow?". This work was supported by NSF Grant EAR93-03402.

Appendix A. The dimensionless parameter λ

The parameter λ is given by

$$\lambda = \frac{2fc}{3\gamma Y(a)} \frac{\mu_2}{\mu_1} \frac{H_0^3}{a^3} \tag{A1}$$

If we assume that R is half the wavelength of the initial undulation, then according to linear Rayleigh–Taylor stability theory (Whitehead and Luther, 1975)

$$R = \pi \left(\frac{\mu_2}{3\mu_1} \right)^{1/3} H_0 \tag{A2}$$

Thus λ becomes

$$\lambda = \frac{2fc}{\pi^3 \gamma Y(a)} \frac{R^3}{a^3} \tag{A3}$$

To determine a numerical range for λ we note that $\gamma = \frac{1}{8}(1 - \epsilon^{-4}) = 0.1227$ and $3 \leq c \leq 2\pi$. An upper limit on f is clearly 1.0. A lower limit on f can be estimated by replacing the Gaussian shaped undulation with a flat-topped cylinder of equal radius and volume and thus a height of $2\gamma h$. Thus the hydrostatic pressure near the edge of the cylinder would be $P_0 - 2\gamma\Delta\rho gh$. We therefore assume that a lower limit on f is $2\ \gamma \approx 0.25$. A reasonable range of a/R is $1/10 \leq a/R \leq 1/2$; a maximum value of $1/2$ for a/R is chosen because the channel flow approximation (in the region outside the undulation) is poor for values of a/R too close to unity. Thus, in the end, we find $10 \leq \lambda \leq 1000$.

Appendix B. Trajectory of the ascending diapir

We desire a simple model to describe the ascent of the plume head or diapir once it separates from the source region. This model is merely appended onto our non-linear model in order to compare to the laboratory experiments. We assume that after separation the diapir rises with a velocity approximately equal to its Stokes velocity; therefore after separation,

$$\frac{h_0}{t_0}\frac{\mathrm{d}h}{\mathrm{d}t} = \frac{\Delta\rho g}{3\mu_2}\left(\frac{3V}{4\pi}\right)^{2/3} \tag{B1}$$

where V is the volume of the diapir, and for simplicity we have neglected the change in thickness of the source region H (assuming it is broad enough that its drainage by the conduit causes a negligible change in H). As the diapir ascends it is inflated by the trailing conduit with a volumetric flux Q which, upon the diapir's separation from the source region, is given by Eq. (27). Thus, assuming Q does not change after separation, $V = Qt_0(t - t_{\mathrm{sep}}) + V_{\mathrm{i}}$ where t_{sep} is the time to separation (obtained by substituting h_{sep} from Eq. (25) into Eq. (21), V_{i} is the initial diapir volume upon separation as given by Eq. (29), and we have neglected the growth in volume of the conduit itself (Olson, 1990). We therefore obtain

$$\frac{\mathrm{d}h}{\mathrm{d}t} = \left[\frac{\alpha}{\lambda}\left(\frac{1+\nu\beta^3}{\beta^3 h_{\mathrm{sep}}}\right)^{1/2}(t - t_{\mathrm{sep}}) + 1\right]^{2/3}\frac{\beta^3 h_{\mathrm{sep}}}{1+\nu\beta^3} \tag{B2}$$

where

$$\alpha = \sqrt{\frac{c^3 R^4 H_0^2}{48 h_0^3 a^3}} \tag{B3}$$

and we have required that

$$\frac{\mathrm{d}h}{\mathrm{d}t} = \frac{\beta^3 h_{\mathrm{sep}}}{1+\nu\beta^3} \quad \text{at} \quad t = t_{\mathrm{sep}} \tag{B4}$$

as given by Eqs. (17) and (25). Evaluation of a (using the appropriate scales from linear stability analysis; see Appendix A) shows that $1 \leq \alpha/\lambda \leq 2$. Eq. (B2) is used to determine h versus t in Fig. 3 after separation has occurred.

References

Batchelor, G.K., 1967. An Introduction to Fluid Dynamics. Cambridge University Press.

Bercovici, D. and Mahoney, J., 1994. Double flood basalts and plume head separation at the 660 kilometer discontinuity. Science, 266: 1367–1369.

Boehler, R., 1993. Core–mantle reactions? Eos Trans. AGU, 74(43), 415.

Cafaro, E. and Cima, C., 1993. Nonlinear analysis of the two-dimensional Rayleigh–Taylor instability. Int. Comm. Heat Mass Transfer, 20: 597–603.

Campbell, I.H. and Griffiths, R.W., 1990. Implications of mantle plume structure for the evolution of flood basalts. Earth Planet. Sci. Lett., 99: 79–93.

Christensen, U., 1984. Instability of a hot boundary layer and initiation of thermo-chemical plume. Annales Geophysicae, 2: 311–320.

Davies, G.F., 1988. Ocean bathymetry and mantle convection, 1. Large-scale flow and hotspots. J. Geophys. Res., 93: 10467–10480.

Farnetani, C.G. and Richards, M.A., 1994. Numerical investigations of the mantle plume initiation model for flood basal events. J. Geophys. Res., 99: 13813–13833.

Farnetani, C.G. and Richards, M.A., 1995. Thermal entrainment and melting in mantle plumes. Earth Planet. Sci. Lett., 136: 251–267.

Fermigier, M., Limat, L. and Wesfried, J.E., 1992. Two-dimensional patterns in Rayleigh–Taylor instability of a thin layer. J. Fluid Mech., 236: 349–383.

Gubbins, D. and Richards, M., 1986. Coupling of the core dynamo and mantle: Thermal or topographic? Geophys. Res. Lett., 13: 1521–1524.

Haan, S.W., 1989. Onset of nonlinear saturation for Rayleigh–Taylor growth in the presence of a full spectrum of modes. Phys. Rev. A, 39: 5812–5825.

Jeanloz, R., 1993. Chemical reactions at Earth's core–mantle boundary: Summary of evidence and geomagnetic implications. In: K. Aki and R. Dmowska (Editors), Relating Geophysical Structures and Processes: The Jeffreys Volume. Geophys. Monogr. Ser., Vol. 76, AGU, Washington, DC, pp. 121–127.

Kull, H.J., 1991. Theory of the Rayleigh–Taylor Instability. Phys. Rep., 206: 197–325.

Kuo, B.Y. and Wu, K.Y., 1995. Large scale shear velocity variations in the D″ layer. EOS Trans. AGU, 76(46): F403.

Larson, R.L. and Olson, P., 1991. Mantle plumes control magnetic reversal frequency. Earth Planet. Sci. Lett., 107: 437–447.

Loper, D.E., 1992. On the correlation between mantle plume flux and the frequency of reversals of the geomagnetic field. Geophys. Res. Lett., 19: 25–28.

Loper, D.E. and Eltayeb, I.A., 1986. On the stability of the D″ layer. Geophys. Astrophys. Fluid Dyn., 36: 229–255.

Loper, D.E. and Lay, T., 1995. The core mantle boundary region. J. Geophys. Res., 100: 6397–6420.

Mahoney, J.J., Storey, M., Duncan, R.A., Spencer, K.J. and Pringle, M., 1993. Geochemistry and age of the Ontong Java Plateau. In: M. Pringle, W. Sager, W. Sliter and S. Stein (Editors), The Mesozoic Pacific: Geology, Tectonics, and Volcanism. AGU Monogr., 77: 233–261.

Nataf, H.-C. and VanDecar, J., 1993. Seismological detection of a mantle plume? Nature, 364: 115–120.

Olson, P., 1990. Hot spots, swells and mantle plumes. In: M.P. Ryan (Editor), Magma Transport and Storage. John Wiley, New York, pp. 33–51.

Olson, P., Schubert, G. and Anderson, C., 1987. Plume formation in the D″-layer and the roughness of the core–mantle boundary. Nature, 327: 409–413.

Ribe, N.M. and de Valpine, D.P., 1994. The global hotspot distribution and instability of D″. Geophys. Res. Lett., 21: 1507–1510.

Richards, M.A., Duncan, R.A. and Courtillot, V.E., 1989. Flood basalts and hot-spot traces: plume heads and tails. Science, 246: 103–107.

Shankland, T.J., Peyronneau, J. and Poirier, J.-P., 1993. Electrical conductivity of the Earth's lower mantle. Nature, 366: 453–455.

Sleep, N., 1990. Hotspots and mantle plumes: Some phenomenology. J. Geophys. Res., 95: 6715–6736.

Turcotte, D.L. and Schubert, G., 1982. Geodynamics: Applications of Continuum Physics to Geological Problems. John Wiley, New York.

Weinberg, R.F. and Podladchikov, Y.Y., 1995. The rise of solid-state diapirs. J. Struct. Geol., 17: 1183–1195.

White, R.S. and McKenzie, D.P., 1989. Magmatism at rift zones: the generation of volcanic continental margins and flood basalts. J. Geophys. Res., 94: 7685–7729.

Whitehead, J.A. and Luther, D.S., 1975. Dynamics of laboratory diapir and plume models. J. Geophys. Res., 80: 705–717.